Hydrogen Bonding in Monomers and Dimers of 2-Aminoethanol

Igor Vorobyov, M. Cecilia Yappert, and Donald B. DuPré*

Department of Chemistry, University of Louisville, Louisville, Kentucky 40292

Received: August 17, 2001; In Final Form: November 9, 2001

Equilibrium structures of monomers and dimers of 2-aminoethanol (AE) exhibiting different intramolecular and intermolecular hydrogen bonds between the OH and NH_2 groups were optimized and analyzed in theoretical density functional B3LYP/6-311++G(2d,2p) calculations. Natural bond orbital (NBO) theory was applied to quantify the relative strength of these interactions and to account for their effect on stability, structural, and vibrational parameters of both monomers and dimers. It is shown that the charge transferred from the lone pair of the hydrogen bond acceptor to the antibonding orbital of the donor provides the substantial stabilizing component of the hydrogen bond. NBO energetic analysis demonstrates that the OH···N interaction is the strongest one for both monomers (intramolecular) and dimers (intermolecular). The intramolecular hydrogen bond in AE monomers is relatively weak, in part, because of its bent nature. The formation of a stronger and more linear intermolecular hydrogen bond between molecular units in AE dimers is accompanied by cooperative enhancement of the intramolecular hydrogen-bonding interactions. This effect is explained in terms of charge transfer among local bond orbitals and is relevant to the cooperative strengthening of hydrogen-bonding interactions in larger AE clusters.

1. Introduction

2-Aminoethanol (AE) or monoethanolamine has been the subject of numerous experimental,[1−11] theoretical,[12−22] and combined studies[23,24] for the past 30 years. Although a relatively simple molecule, the AE moiety is an important constituent of some biologically relevant molecules such as phospholipids (as the headgroup of phosphatidylethanolamine).

Two types of intramolecular hydrogen bonds, OH···N and NH···O, can be formed in this molecule. Microwave,[8,9] infrared,[3,4,23] and photoelectron[6] spectroscopic studies showed that this molecule exists predominantly in the gas phase as the gauche conformer (with respect to the rotation around the C−C bond), which is stabilized by an OH···N intramolecular hydrogen bond. The formation of this bond influences structural[8,9] and spectroscopic[3,4,23] parameters of the molecule. These experimental findings were confirmed by ab initio calculations[13,15−17,19,21−24] at different levels of theory ranging from Hartree−Fock (HF) with the small STO-3G basis set up to Møller−Plesset second-order perturbation theory (MP2) with the extended 6-311+G(2d,p) basis set. Most theoretical studies have focused on the influence of basis set and electron correlation on the order of stability and structural parameters of AE conformers,[16,22] comparison of experimental and calculated gas-phase vibrational spectra of AE,[23] calculation of rotational barriers between different AE conformers,[13] evaluation of energetic contributions for intrinsic gauche and hydrogen-bonding interactions.[15] However, the analysis of localized orbital interactions in monomers and dimers of AE has not been reported so far.

Both infrared spectroscopic data[23] and molecular dynamics simulation[14] suggest the disruption of intramolecular hydrogen bonds during the formation of intermolecular OH···N hydrogen bonds in neat liquid AE. The translational and rotational mobility (neat liquid AE) as found by ^1H and ^{13}C NMR T_1 measurements[1,10] also correlates with the formation of a hydrogen-bonding network. The formation of dimers has been inferred from H^+ potentiometric titrations[7] in dilute aqueous solution of AE. In this case, a cyclic structure with two equivalent intermolecular hydrogen bonds of the OH···N type was proposed to be most prevalent. However, the possible formation of different homo- and heteroconjugates with both ring and chain structures was also mentioned.[7]

The crystal structure of AE was determined from X-ray spectroscopy by Mootz et al.[11] In crystalline AE, the molecules are in the *trans*-conformation (with respect to the rotation around the C−C bond) and linked through intermolecular OH···N and NH···O bonds into angular chains.[11]

To our knowledge, theoretical studies on AE clusters, except for the molecular dynamics simulations mentioned above,[14] have not been performed so far. Ab initio studies can be of value in describing the competition between inter- and intramolecular hydrogen bonds and the cooperative character of such interactions. Many studies on clusters of other molecules capable of intermolecular hydrogen bond formation have been reported.[25−30] However, high-level computational studies of molecular complexes where both inter- and intramolecular hydrogen bonds are present are relatively rare.[31,32]

This study focuses on the conformational analysis of isolated molecules of AE as well as selected AE dimers by using density functional theory (DFT) and an extended basis set, with the main emphasis on the intra- and intermolecular hydrogen-bonding interactions. Natural bond orbital (NBO) theory was applied to analyze hydrogen-bonded conformers in terms of orbital interactions. NBO analysis has been successfully applied to a number of other systems including ones with intramolecular hydrogen bonds[33,34] and molecular clusters where intermolecular hydrogen bonding takes place.[29,35−41] No NBO studies concerning hydrogen-bonding interactions in AE or other amino alcohols have been performed so far.

* Corresponding author. E-mail address: d.dupre@louisville.edu.

10.1021/jp013211e CCC: $22.00
Published on Web 01/08/2002

2. Computational Methods

All calculations were performed using Gaussian 98[42] electronic structure package. Geometry optimizations of AE conformers were performed using DFT with the B3LYP hybrid functional[43,44] and the 6-311++G(2d,2p) extended, split-valence, triple-ζ basis set with two sets of polarization functions and diffuse orbitals on all atoms, including hydrogens. It is well-known that the inclusion of electron correlation as well as the use of flexible, extended basis sets with diffuse functions is necessary for the accurate description of hydrogen-bonding interactions.[45−49] B3LYP/6-311++G(2d,2p) calculations were successfully applied by Lii et al.[50] to hydrogen-bonded systems such as the water dimer and carbohydrates, by Lundell et al. to water−carbon monoxide complex,[51,52] and by Przeslawska et al.[53] to other amino alcohols: 3-(dimethylamino)-1-propanol and 3-amino-1-propanol.

Force constants were calculated analytically at the first step of optimization. Geometries of AE dimers were first optimized with HF/6-31G(d,p) and then B3LYP/6-31G(d,p) calculations. The final molecular geometries, used throughout this study, were obtained at the B3LYP/6-311++G(2d,2p) level of theory. Frequency calculations for AE monomers and dimers were performed at the same level of theory. Stationary points were identified as local minima by the absence of imaginary frequencies.

The interaction energy of AE dimers, defined as the difference between the energy of the complex and that of isolated monomers (in the geometry of the complex), was calculated at HF, B3LYP, and MP2 (frozen-core approximation) levels of theory with the 6-311++G(2d,2p) basis set for B3LYP/6-311++G(2d,2p) optimized structures. Basis set superposition error (BSSE) was corrected by the counterpoise (CP) method of Boys and Bernardi.[54] This correction can be overestimated for correlated methods.[55] Therefore, both corrected values of interaction energies and the BSSE are reported below. The deformation energy, defined as the energy required to distort the equilibrium geometry of an isolated monomer to that found in the complex, was also added as a correction. The difference in the zero-point vibrational energy between the AE dimer and isolated monomers is also given. For all single-point energy calculations, the SCF = Tight option was used as the basis set contains diffuse functions.

A thorough conformational analysis of optimized AE monomers and dimers was performed at the B3LYP/6-311++G(2d,2p) level by using NBO theory,[56] including natural population analysis (NPA),[57] natural steric analysis (NSA),[58] and natural resonance theory (NRT).[59−62] The NBO 4.0 program[63] linked to Gaussian 98 was used for these calculations.

NBO analysis allows the transformation of canonical molecular orbitals into an orthonormal set of one- and two-center-localized orbitals (NBOs) analogous to traditional Lewis-type orbitals. Sparsely occupied, nonideal antibonding and Rydberg orbitals also arise and act as depositories of conformationally dependent inter- and intramolecular electron charge transfers (CT).[56] Quantitative estimate of these electron delocalizations can be made by deletion of specific off-diagonal $<a|F|b>$ matrix elements of the effective one-electron Hamiltonian (Fock or, in DFT, Kohn−Sham matrix) in the NBO basis and subsequent recalculation of the electronic energy.[56] It is also possible to estimate the energy lowering, $E^{(2)}$, caused by CT interactions by performing second-order perturbation analysis.[37,56] $E^{(2)}$ values are directly proportional to the overlap integral, S(a,b), between pre-orthogonalized NBOs (pre-NBOs) and inversely proportional to the energy difference between corresponding NBOs.[37,41,56] NSA provides a numerical estimate of steric exchange repulsions from the energy of orthogonalization of pre-NBOs.[58] NRT analysis allows the determination of the leading resonance structure or structures for the molecules and provides resonance-weighted bond orders that are useful in the determination of relative bond strength and partial double-bond character for single bonds.[60−62] The numerical Fletcher−Powell (FP) optimization procedure[64] incorporated in Gaussian 98 was also used to reoptimize geometries in the absence of specific charge-transfer interactions.[63]

The notation used in this work for categorizing the conformers of AE is the same as that used by Radom et al.[19] Here a general conformer is represented as *xYz*, where ***x*** designates the value of the *H−O−C−C* dihedral angle; ***Y***, the *O−C−C−N* dihedral angle; and ***z***, the *lpN−N−C−C* dihedral angle. *lpN* denotes the lone pair on the nitrogen atom. The one-letter abbreviations are: A or a for anti-clinal, G or g for gauche(+) {(+)syn-clinal}, G′ or g′ for gauche(−) {(−)syn-clinal}, S or s for syn-periplanar; T or t for *trans* {anti-periplanar}. In this study we report two *H−N−C−C* dihedral angles instead of just the *lpN−N−C−C* one. When looking along the N−C axis and rotating the molecule so that the lone pair on N is on the top, the H atom of the NH_2 group which is on the right will be called H_a, and the one on the left will be called H_b.

The general notation used in this study for the hydrogen bond is AH···B where A is the hydrogen bond donor (oxygen or nitrogen) and B is the hydrogen bond acceptor (oxygen or nitrogen). A hydrogen bond is considered to be formed when the corresponding internuclear distance, r(AH···B), is within the sum of van der Waals radii (using values recommended by Bondi[65]) of H and the hydrogen bond acceptor atom B; i.e., 2.75 Å for OH···N and NH···N interactions, and 2.72 Å for NH···O and OH···O interactions.

3. Results and Discussion

This section presents the results and discussion of the analysis of hydrogen-bonding interactions in AE monomers first and then in dimers.

3.A. Choice of Basis Set and Level of Theory. The choice of the proper basis set and the level of theory is critical in conformational analysis. The study on AE by Kelterer et al.[16] and some earlier studies[21,24] have shown that the basis set influences not only the order of stability of conformers, but also the number of local minima. The latter effect is related to the very low potential energy barriers for the internal rotation for some AE conformers.[16] Also, the inclusion of electron correlation by virtue of MP2 influences the relative energy differences and structural parameters of AE conformers.[16,22]

Another important aspect is the correspondence between theory and experiment. The geometrical parameters and the dipole moment of the global minimum of AE can be compared with corresponding experimental values obtained from microwave spectroscopy[8,9] and subjected to critical evaluation and compilation[66] (see Table 1). Most of the experimental structural data have relatively large uncertainties and represent so-called effective parameters (r_0), which are physically not well defined and based on several assumptions.[66] This precludes a rigorous evaluation of calculated parameters, which are equilibrium parameters (r_e). Nevertheless, a semiquantitative assessment of the computational method and basis set quality for the conformational analysis still may be performed with such comparisons. This is especially true for hydrogen-bonding parameters critical for our study and obtained experimentally as substitution (r_s) parameters, which usually match equilibrium structures closer

TABLE 1: Calculated and Experimental Values for Selected Geometric Parameters and Dipole Moments for the Lowest Energy Conformer (g′Gg′) of 2-Aminoethanol

		calculations (basis set and theoretical level)					
		6-31G(d,p)			6-311++G(2d,2p)		
	experiment[a]	HF	B3LYP	MP2[b]	HF	B3LYP	MP2
bond lengths[c]							
C−C	*1.526 ± 0.016*	1.521	1.530	1.521	1.516	1.524	1.518
C−O	*1.396 ± 0.010*	1.394	1.412	1.416	1.396	1.419	1.421
C−N	*1.475 ± 0.023*	1.457	1.471	1.468	1.457	1.471	1.470
O−H	***1.000 ± 0.020***	0.946	0.973	0.971	0.942	0.966	0.965
N−H_a	***1.017 ± 0.003***	0.999	1.015	1.013	0.996	1.011	1.009
N−H_b	***1.017 ± 0.005***	1.001	1.018	1.015	0.998	1.013	1.011
nonbonding distances[c]							
r(O···N)	***2.808 ± 0.005***	2.820	2.773	2.762	2.860	2.827	2.797
r(OH···N)	***2.300 ± 0.040***	2.325	2.181	2.175	2.402	2.293	2.246
bond angles[d]							
C−C−O	*112.1 ± 1.0*	111.3	110.6	110.2	111.9	111.4	110.7
C−C−N	*108.1 ± 2.0*	109.1	108.1	107.6	109.8	109.0	108.0
C−O−H	*108.0 ± 2.0*	107.1	103.8	103.5	108.1	105.8	104.8
C−N−H_a	*110.4 ± 0.8*	111.7	111.1	110.7	111.7	111.6	111.4
C−N−H_b	*111.3 ± 0.8*	111.2	110.4	109.8	111.3	111.2	110.6
H−N−H	***109.9 ± 0.5***	107.5	106.8	106.5	107.5	107.4	106.9
dihedral angles[d]							
O−C−C−N	*55.4 ± 2.0*	57.9	53.7	55.3	59.9	56.3	57.1
C−C−O−H	*−27.0 ± 6.0*[e]	−43.7	−39.2	−40.6	−45.2	−41.3	−41.8
C−C−N−H_a	*−159.5 ± 1.0*	−163.1	−162.5	−164.0	−163.9	−161.4	−163.6
C−C−N−H_b	*78.2 ± 2.0*	76.8	79.2	78.6	75.9	78.7	77.6
μ (debyes)	*3.05 ± 0.05*	3.20	3.20	3.49	3.04	3.10	3.30

[a] Microwave spectroscopy. Data from refs 8 and 9 subjected to critical evaluation in ref 66 are used. Effective (r_0) parameters are given in *italic* whereas substitution (r_s) parameters are given in ***bold italic***. The uncertainties given in the original experimental papers are kept except for values of N−H_a and C−C−O for which larger error estimates from ref 66 are given. [b]See also ref 13. [c]All bond lengths and distances are given in angstroms. [d]All angles and dihedral angles are given in degrees. [e]Probably unreliable. See ref 66.

than r_0.[66] For comparison, we used two basis sets, 6-31G(d,p) and 6-311++G(2d,2p), and three theoretical levels: HF, MP2, and DFT (B3LYP hybrid functional). The values of some calculated (r_e) and experimental (r_0 and r_s) parameters are summarized in Table 1.

In agreement with previous studies,[47,48] the inclusion of electron correlation is necessary to obtain values of structural parameters close to experimental values. However, the use of the relatively small 6-31G(d,p) basis set at B3LYP or MP2 level tends to overestimate the strength of the hydrogen bond. The more extended 6-311++G(2d,2p) basis set yields improvement. MP2 calculations with this basis set are very computationally expensive and become impractical for larger systems, such as AE clusters. B3LYP/6-311++G(2d,2p) calculations, however, are affordable for geometry optimizations and frequency calculations of both AE monomers and dimers. In agreement with previous studies (see above), the optimized geometry and dipole moment of the g′Gg′ conformer produced by this method match well with experimental values. The B3LYP/6-311++G (2d,2p) combination was therefore used to analyze hydrogen-bonding interactions in AE monomers and dimers.

3.B. Monomer Studies. *3.B.1. Energies and Relative Populations of Stable Conformers.* AE is a three-rotor molecule in which rotation around C−C, C−O, and C−N bonds may take place. This means that 27 noneclipsed conformers are possible, 14 of which are nonequivalent. B3LYP/6-311++G(2d,2p) conformational analysis located 13 nondegenerate stationary states on the potential energy surface of AE in agreement with previous studies.[13,15,22,23] The equilibrium structure corresponding to the g′Gg conformer was not located. Relative energies of these conformers are given in Table 2. The g′Gg′ conformer is the global minimum and exhibits an OH···N intramolecular hydrogen bond. The gGg′ conformer with the same type of hydrogen bond and the NH···O hydrogen-bonded conformers gGt, tGt, tGg, and gGg follow with higher energies. The addition of zero-point vibrational energy and thermal corrections to the electronic energy, and the inclusion of the entropic factor, decreased the energy gap between conformers and also switched the order of stability for some. All hydrogen bonded conformers, shown in Figure 1, however, exhibited lower energies than non-hydrogen-bonded ones. This indicates that the intramolecular hydrogen bond has a substantial effect on the conformational stability of AE. Relative populations, based on the Boltzmann distribution, were calculated with zero-point corrected electronic energy and are also shown in Table 2. They indicate that g′Gg′

TABLE 2: B3LYP/6-311++G(2d, 2p) Calculated Relative Energies, Populations, and Dipole Moments for Stable Conformers of 2-Aminoethanol

	ΔE[a]	ΔE_0[b]	ΔH[c]	ΔG[d]	%[e]	μ[f]
g′Gg′	0.00	0.00	0.00	0.00	63.37	3.10
gGg′	1.57	1.31	1.56	0.76	6.92	2.09
gGt	1.57	1.27	1.44	1.10	7.46	0.98
tGt	1.75	1.37	1.56	1.16	6.32	2.63
tGg	1.90	1.57	1.73	1.41	4.45	1.41
gGg	1.92	1.64	1.77	1.53	3.95	2.51
tGg′	2.31	1.91	2.08	1.72	2.54	1.48
tTg	2.73	2.31	2.56	2.06	1.29	1.45
tTt	2.79	2.27	2.56	1.96	0.69	2.60
gTt	2.85	2.39	2.71	2.04	1.11	0.99
gTg	2.90	2.51	2.78	2.21	0.92	1.65
g′Tg	2.97	2.53	2.80	2.24	0.89	2.69
g′Gt	4.59	3.86	4.26	3.26	0.09	2.23

All energies are in kilocalories per mole relative to the most stable conformer (g′Gg′) for which: [a]Electronic energy (E) is −210.471970 au, [b]sum of electronic and zero-point energy (E_0) is −210.373604 au, [c]sum of electronic and thermal enthalpy (H) at 298 K is −210.367575 au, [d]sum of electronic and thermal free energy (G) is −210.400882 au. [e]Relative populations (%) at 298 K are calculated from ΔE_0 based on the Boltzmann distribution. [f]Dipole moments (μ) are in debyes.

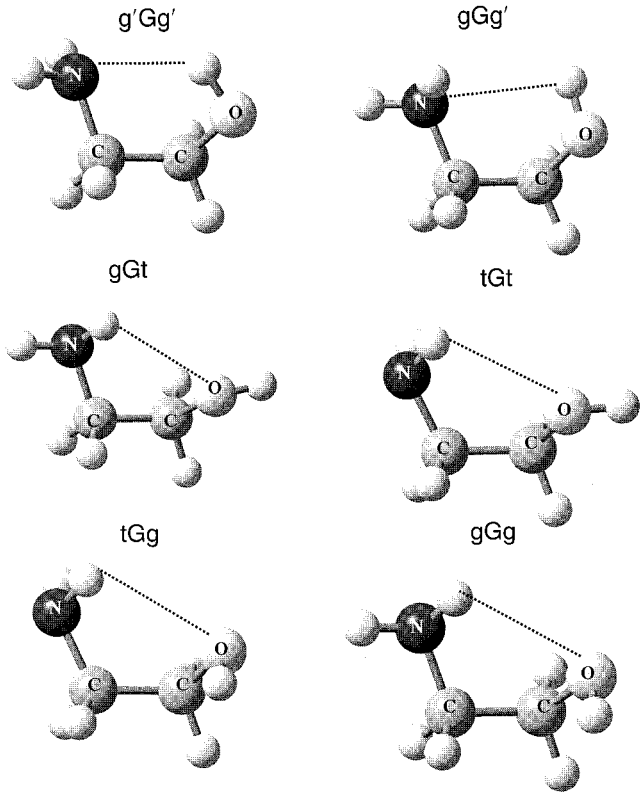

Figure 1. Stable conformers of AE with OH···N (g′Gg′ and gGg′) and NH···O (gGt, tGt, tGg, and gGg) intramolecular hydrogen bonds. These structures were optimized at the B3LYP/6-311++G(2d,2p) level.

is the predominant conformer in the gas phase at 298 K. This is in excellent agreement with earlier computational studies[13,15−23] and experimental data from microwave[8,9] and infrared spectroscopy.[23] Structural and energetic parameters associated with the intramolecular hydrogen bond in the six AE conformers are presented in Table 3.

3.B.2. Structural Parameters of the Intramolecular Hydrogen Bond. As indicated in previous studies,[17,22] envelope-type five-membered rings are formed in AE conformers with both OH···N and NH···O intramolecular hydrogen bonds. Such hydrogen bonds are therefore bent, and corresponding ∠O−H···N and ∠N−H···O angles are far from the "ideal" 180°.

The geometric parameters in Table 3 clearly demonstrate that the OH···N hydrogen bond in g′Gg′ is much stronger than that in gGg′ and the NH···O interaction for gGg, gGt, tGg, and tGt. Structural parameters alone, however, cannot arrange with certainty NH···O hydrogen-bonded conformers by the hydrogen bond strength. For instance, the gGt conformer has smaller H···O and N···O internuclear distances, but the gGg conformer has the greater value of ∠N−H···O. Therefore, some criterion based on energy (discussed below) is necessary to evaluate the relative strength of hydrogen-bonding interactions.

3.B.3. Energetics of the Intramolecular Hydrogen Bond from NBO Analysis. NBO theory describes the formation of a AH···B hydrogen bond as the CT from the lone pair, n(B), of the base B into the vacant antibonding orbital σ^*(AH) of the acid A. NBO analysis for AE places one lone pair on the N atom and two nonequivalent symmetry-adapted lone pairs on the O atom. The lone pair on nitrogen, n(N), is a sp^x ($x \sim 4.2$) hybrid pointing outward from the apex N of the trigonal pyramid defined for CNH_2. One of oxygen lone pairs, n_{sp}(O), is also a sp^x ($x \sim 1.1$) hybrid, lying along the bisector of C−O−H angle with the large lobe pointing outward. The other oxygen lone pair, n_p(O), lies perpendicular to the C−O−H plane and is almost a pure p-type orbital.

The remote n(B)→σ^*(AH) delocalization leads to energy lowering that can be quantified by the $E^{(2)}$ values (see above). These numbers can be used to estimate the relative strength of hydrogen bonds. $E^{(2)}$ values in Table 3 demonstrate that the n(N)→σ^*(OH) interaction in the g′Gg′ conformer is eight times more effective than that in gGg′. The overlap of the n(N) orbital with σ^*(OH) for the g′Gg′ conformer is shown in the upper panel of Figure 2. It is seen that the antibond is more polarized toward N and is asymmetric around the O−H axis. This results in a more effective overlap with n(N) which favors CT. Both lone pairs on the oxygen atom can participate in n(O)→σ^*(NH) CT interactions upon NH···O hydrogen bond formation. $E^{(2)}$ values in Table 3 clearly demonstrate that the interaction of the p-type oxygen lone pair is much more effective than that for the sp-type oxygen lone pair. This is due to both greater overlap, $S(n,\sigma^*)$, and the smaller NBO energy difference, $\Delta\epsilon(n,\sigma^*)$, for n_p(O). Overlaps of both lone pairs on the oxygen atom with σ^*(NH) for the gGg conformer of AE are shown in the top panels of Figure 3.

Deletion energies, $E_{del}(n\rightarrow\sigma^*)$, for intramolecular n(B)→σ^*(AH) CT interactions (from both oxygen lone pairs for the NH···O hydrogen bond) are also listed in Table 3. These values are comparable to those calculated for $E^{(2)}$. To estimate the relative strength of hydrogen-bonding interactions among all conformers, the energy change associated with deletion of all five such CT interactions [one n(N)→σ^*(OH) and four n(O)→σ^*(NH) from both oxygen lone pairs and to both N−H antibonding orbitals], E_{HB}, was also calculated (see Table 3). It is clear that the g′Gg′ conformer is stabilized the most by the formation of the intramolecular hydrogen bond. For all NH···O hydrogen-bonded conformers, E_{HB} is much lower. One can also see that the gGt conformer has a weaker hydrogen bond than the gGg conformer, a fact that is unclear from the comparison of the corresponding hydrogen bonding distances and angles alone.

The relative strength of OH···N and NH···O intramolecular hydrogen bonds can be accounted for by the electronegativity difference between nitrogen and oxygen. Because polarization is reversed in the antibonding orbitals, more electron density is around hydrogen in σ^*(OH) (74.3% for g′Gg′) than in σ^*(NH) (68.3% for gGg). This makes $S(n,\sigma^*)$ overlap more effective for the OH···N hydrogen bond. In addition, nitrogen, being more electropositive, is a better electron donor than oxygen, further enhancing the OH···N interaction relative to the NH···O one.

Besides n(B)→σ^*(AH) delocalizations, other factors such as electrostatic, polarization, dispersion interactions result in the net stabilization of the AH···B hydrogen-bonding contact. NBO theory does not provide a separate numerical estimate for these components. Using a completely different approach, Chang et al.[15] estimated the electrostatic component of the intramolecular hydrogen bond to be 3.67 kcal/mol for the g′Gg′ conformer and 0.77 kcal/mol for the gGt conformer. This stabilization effect is higher than our estimate from CT interactions as found with NBO theory. However, the charge distribution on the atoms of any AE conformer can be viewed as a consequence of internal delocalizations, which may modulate electrostatic interactions making them more favorable.

A concurrent force of destabilization of the hydrogen bond is steric exchange repulsion between mostly filled n(B) and σ(AH) orbitals, n(B)↔σ(AH). Corresponding values for overlap integrals, $S(n,\sigma)$, and pairwise exclusion repulsion energies, $dE(n,\sigma)$, derived from NSA, also are given in Table 3. For the g′Gg′ conformer, the stabilization caused by n(N)→σ^*(OH) CT

TABLE 3: Values for Structural and Energetic Parameters Associated with Intramolecular Hydrogen Bond Formation for Stable Conformers of 2-Aminoethanol. B3LYP/6-311++G(2d,2p)//B3LYP/6-311++G(2d,2p) Calculations

	g′Gg′	gGg′	gGg	gGt	tGg	tGt
AH···B	OH···N	OH···N	NH···O	NH···O	NH···O	NH···O
			structural parameters[a]			
r(A···B)	2.827	2.870	2.934	2.876	3.005	2.943
r(AH···B)	2.293	2.580	2.568	2.533	2.636	2.600
∠(A−H···B)	114.0	97.6	100.9	99.3	101.4	99.6
			energetic parameters			
n(B)→σ*(AH)[b]						
$S(n,\sigma^*)$[c]	0.1281	0.0382	0.0133/−0.0399	0.0199/0.0308	0.0080/−0.0336	0.0193/0.0195
$\Delta\epsilon(n,\sigma^*)$, au[d]	0.78	0.76	1.06/0.75	1.07/0.76	1.06/0.75	1.07/0.76
$E^{(2)}$, kcal/mol	2.00	0.25	0.02/0.30	0.06/0.15	0.01/0.26	0.06/0.08
n(B)↔σ(AH)[b]						
$S(n,\sigma)$[c]	0.1013	0.0426	0.0146/−0.0620	0.0342/0.0477	0.0117/−0.0544	0.0353/0.0317
$dE(n,\sigma)$[e]	2.47	0.38	0.08/0.69	0.22/0.53	0.06/0.53	0.24/0.26
deletion energies[f]						
E_{HB}	2.59	0.52	0.43	0.32	0.33	0.21
$E_{del}(n\rightarrow\sigma^*)$	2.53	0.32	0.37	0.24	0.31	0.16

[a] All distances are in angstroms; angles are in degrees. [b]For conformers with the NH···O intramolecular hydrogen bond, the charge transfer and exchange repulsion with both lone pairs on the oxygen atom are given and separated by a slash [n_{sp}(O)/n_p(O)]. [c]Overlap integral of associated pre-orthogonalized NBOs. [d]NBO energy difference between n and σ*. [e]Exclusion repulsion energy (kilocalories per mole) between n and σ. [f]Energy change (in kilocalories per mole) associated with deletion of off-diagonal matrix elements of effective one-electron Hamiltonian corresponding to: either one *n(N)→σ*(OH)* or two *n(O)→σ*(NH)* charge-transfer interactions, denoted as $E_{del}(n\rightarrow\sigma^*)$; all five such interactions [for both *n(O)* and both *σ*(NH)*], taken together, denoted as E_{HB}.

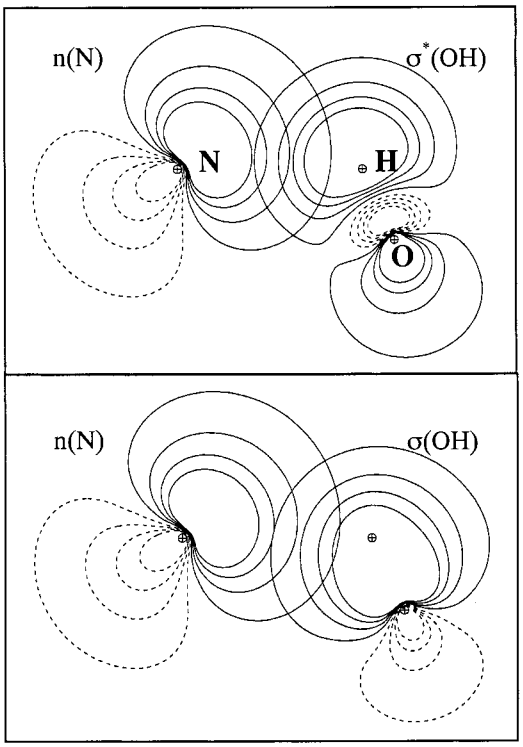

Figure 2. Contour plots of the overlap of pre-orthogonalized natural bond orbitals (pre-NBOs): nitrogen lone pair n(N) with OH antibonding orbital σ*(OH) (top) and OH bonding orbital σ(OH) (bottom) of the g′Gg′ conformer of AE. B3LYP/6-311++G(2d,2p)//B3LYP/6-311++G (2d,2p) calculations. Atomic positions are indicated by circled crosses. The relative positions of atoms are the same on both plots. The outermost contours are at 0.032 au, and the contour interval is 0.05 au.

interaction is expected to be greater than the destabilizing effect of n(N)↔σ(OH) steric exchange repulsion because the $S(n,\sigma^*)$ overlap is greater than $S(n,\sigma)$ (see Table 3 and the lower panel of Figure 2). For gGg′ and all NH···O hydrogen bonded conformers the opposite is true (see Table 3 and bottom panels of Figure 3). Total steric exchange energy is higher for hydrogen-bonded AE conformers, being the highest for g′Gg′ (172.7 kcal/mol), whereas it is only 163.1 kcal/mol for the tGg′ conformer. This is an indication that both OH···N and NH···O intramolecular hydrogen bonds with five-membered ring formed by connected atoms are very strained.

n(B)→σ*(AH) is not the only, and by far not the strongest, intramolecular CT interaction in the AE molecule. Indeed, $E_{del}(n\rightarrow\sigma^*)$ comprises only about 2% of the so-called NOSTAR, or no antibond occupancy, energy of 127 kcal/mol for g′Gg′. About 97% of all CT interactions (in the energetic equivalent) are vicinal delocalizations, which are most effective when corresponding bonding and antibonding or lone pair and antibonding orbitals are periplanar to each other. These interactions may modulate remote n(B)→σ*(AH) delocalizations or may be modulated by them. Their complex interplay affects the values of structural parameters, which is discussed next.

3.B.4. Changes in Structural and Vibrational Parameters across the Hydrogen-Bonded Conformers. The most important structural parameters for all stable AE conformers are listed in Table S1 of the Supporting Information. A comparison of these parameters for the hydrogen-bonded AE conformers was made with those without an intramolecular hydrogen bond as well as with the corresponding parent molecules, i.e., ethanol and ethylamine optimized at the same level of theory (see Table S2 of the Supporting Information). The latter comparison was suggested to us by the work of Varnali and Hargittai[67] on 2-nitroethanol and 2-nitrovinyl alcohol. The most significant changes are observed for the g′Gg′ conformer with the stronger OH···N intramolecular hydrogen bond. The O−H bond is lengthened by ca. 0.006 Å and the C−O−H angle is contracted by ca. 3° compared with ethanol and non-hydrogen-bonded AE conformers. The calculated frequency of the OH stretching normal mode, ν(OH), is red-shifted by 82−106 cm^{-1} with an intensity increase by a factor of 1.7−3.0. These changes are smaller for the other OH···N hydrogen-bonded conformer, gGg′.

NBO theory allows us to account for these differences. The lengthening of the OH bond and corresponding red shift of the ν(OH) frequency for the g′Gg′ conformer is a corollary of the weakening of this bond brought on by the population of the σ*(OH) antibonding orbital during n(N)→σ*(OH) CT. This interaction "softens" this bond, and the corresponding force constant is smaller. Indeed, the occupancy of σ*(OH) for g′Gg′

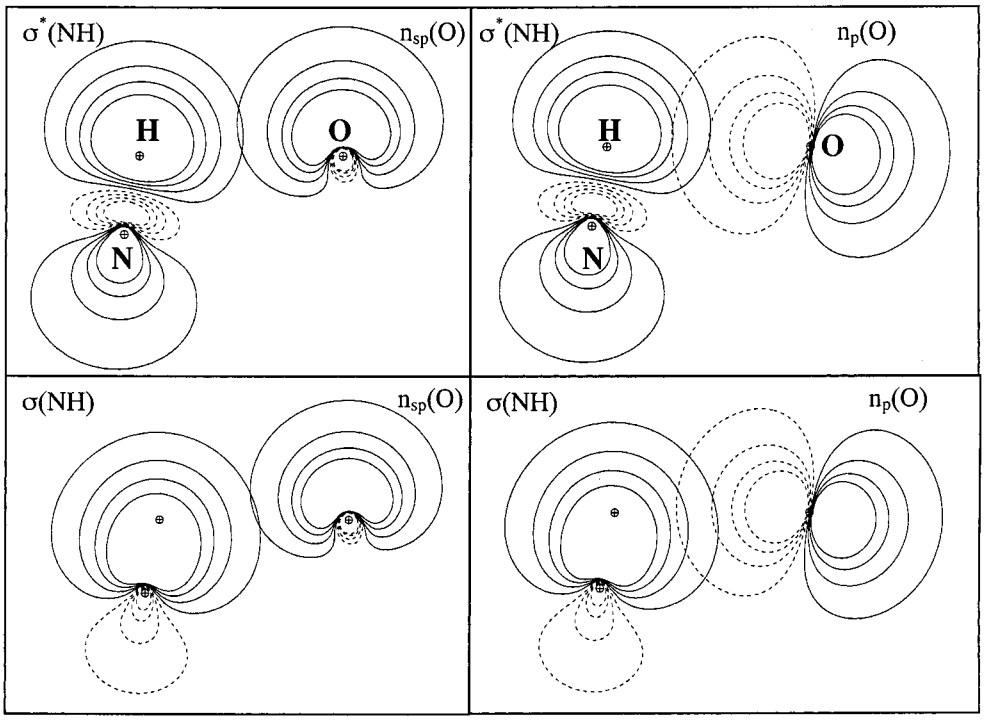

Figure 3. Contour plots of the overlap of pre-orthogonalized natural bond orbitals (pre-NBOs): oxygen lone pairs n_{sp}(O) (left) and n_p(O) (right) with NH_a antibonding orbital $\sigma^*(NH_a)$ (top) and NH_a bonding orbital $\sigma(NH_a)$ (bottom) of the gGg conformer of AE. B3LYP/6-311++G(2d,2p)//B3LYP/6-311++G(2d,2p) calculations. Atomic positions are indicated by circled crosses. The relative positions of atoms are the same on all plots. The outermost contours are at 0.032 au, and the contour interval is 0.05 au.

is the greatest among all AE conformers (0.0148e) and the NRT natural bond order of the O−H bond is the lowest (0.988). The contraction of the C−O−H angle for this conformer, compared with others, which is necessary for the effective n(N)→σ^*(OH) delocalization, can be viewed as a compromise between this favorable CT interaction and σ(OH)↔σ(CO) exchange repulsion. The increase in intensity of the ν(OH) may be also attributed to this CT interaction. The IR intensity is related to the square of the derivative of the electric dipole moment with respect to the atomic displacement along the corresponding normal mode eigenvector.[29] n(N)→σ^*(OH) CT further polarizes the OH bond and produces larger dipole differences with respect to the same atomic displacement. This results in the increase in infrared intensity.

Calculated frequencies for the g′Gg′ conformer are in agreement with experimental values[23] when scaled by a factor of 0.9613 as done by Przeslawska et al.[53] for similar molecules with B3LYP/6-311++G(2d,2p) calculations. For instance, the scaled calculated value of 3606 cm^{-1} for ν(OH) is close to the experimental value[23] of 3570 cm^{-1}; 3455 cm^{-1} calculated for $\nu_{as}(NH_2)$ is close to the experimental value[23] of 3422 cm^{-1}; 3378 cm^{-1} calculated for $\nu_s(NH_2)$ is close to the experimental value[23] of 3356 cm^{-1}.

The changes in structural and vibrational parameters attributed to the formation of the NH···O intramolecular hydrogen bond are minor compared with those related to the OH···N interaction and do not correlate with the hydrogen bond strength (see above). For all NH···O hydrogen-bonded AE conformers the relevant C−N−H angle is contracted by 0.7−1.0°, whereas the length of the relevant N−H bond (participating in the hydrogen bond formation) and frequencies of NH_2 group stretching modes of vibration, $\nu_{as}(NH_2)$ and $\nu_s(NH_2)$, are practically the same as the corresponding values for ethylamine. Among all AE conformers, tGg and tGt, with the weakest NH···O interaction, have the longest N−H bonds and most red-shifted $\nu_{as}(NH_2)$ and $\nu_s(NH_2)$ frequencies. Intensities of these normal modes of vibration are very low, but somewhat higher for all hydrogen-bonded AE conformers.

NBO theory explains the lack of correlation between the hydrogen bond strength and structural and vibrational changes for NH···O bonded conformers by the relative unimportance of the remote n(O)→σ^*(NH) CT compared with vicinal σ→σ^* delocalizations coming from σ(NH) and vicinal σ→σ^* delocalizations going into σ^*(NH). The latter total σ(NH)/σ^*(NH) interactions are greater when the lone pair on nitrogen is *trans* to the C−C bond (cf. deletion energies are 14.7 and 12.8 kcal/mol for tGg and gGg, respectively), which is in agreement with observed trends in structural and vibrational parameters.

The CT nature of the intramolecular hydrogen bond affects other routes of electron delocalization in AE molecule that also lead to changes in structural parameters. Such effects would not be observed if electrostatic interactions alone were responsible for the formation of hydrogen bonds. The most striking example is the variation in C−O and C−N bond lengths. The C−O bond is the shortest for g′Gg′ (1.419 Å) and longest for the gGt conformer (1.433 Å). The opposite is true for the C−N bond. On the basis of NBO theory, the contraction of the C−O bond for g′Gg′ is the consequence of increased vicinal CT interactions of lone pairs on the oxygen atom (deletion energy is 29.3 kcal/mol). These delocalizations occur across the axis of this bond, thereby building partial π-character and making it stronger and shorter. Indeed, C−O has the highest NRT natural bond order for g′Gg′ (1.029). The increased vicinal delocalization of both n(O)s is a corollary of the remote n(N)→σ^*(OH) CT interaction, which brings more electron density onto the oxygen atom, facilitating its further transfer. By the same mechanism, the C−O bond becomes weaker for AE conformers with a NH···O intramolecular hydrogen bond due to decreased vicinal CT from n(O)s; the deletion energy is just 25.3 kcal/mol for gGt. Increased vicinal delocalizations of

corresponding lone pair(s) is another factor that makes hydrogen-bonded conformers more stable relative to non-hydrogen-bonded ones.

3.B.5. Energetic and Structural Parameters of Deletion-Optimized Conformers as a Marker for the Net Effect of Intramolecular Hydrogen-Bonding Interactions. A net estimate of the role of $n(B)\rightarrow\sigma^*(AH)$ charge-transfer interactions can be accomplished by deletion of specific $<n|F|\sigma^*>$ matrix elements during a reoptimization of the molecular geometry of a conformer.[37,63] The CT component of a hydrogen bond can thus be totally eliminated or "turned off" without resorting to artificial and arbitrary bond rotations or energy comparisons with non-hydrogen-bonded conformers. The electronic energy difference between the equilibrium and deletion-optimized structure may then serve as a measure of stabilization due to the CT component of an intramolecular hydrogen bond. This energy change amounts to 0.56 kcal/mol for the g′Gg′ conformer, and it is an order of magnitude smaller for other hydrogen-bonded AE conformers (e.g., 0.06 kcal/mol for gGg and even smaller for others). These numbers indicate that the OH···N intramolecular hydrogen bond in g′Gg′ is stronger and has a greater CT component.

For the $<n(N)|F|\sigma^*(OH)>$ deletion-optimized structure of g′Gg′, the H···N distance is increased by 0.322 Å and the corresponding ∠O−H···N angle is decreased by 10.2° relative to the equilibrium structure. As a result of the elimination of the $n(N)\rightarrow\sigma^*(OH)$ interaction during geometry optimization, the O−H bond is contracted by 0.006 Å. The C−O−H angle widens by 2.6°, which in turn decreases steric exchange repulsions. Deviation of dihedral angles from the ideal staggered values for the deletion-optimized structure is decreased, e.g., by 13.1° for C−C−O−H.

The structural changes for $<n(O)|F|\sigma^*(NH)>$ deletion-optimized structures of AE conformers with the NH···O hydrogen bond are much less significant. For the gGg conformer with the strongest hydrogen bond of this type, the H···O distance is increased by only 0.090 Å. The value of the N−H···O angle is decreased by 3.5°. The N−H bond involved in the hydrogen bond is shortened by 0.002 Å, and the corresponding C−N−H angle widens by 1.1°. Both C−C−N−H dihedral angles become closer to the ideal staggered values by ∼5°. This is yet another evidence of the relative weakness and structural insignificance of the NH···O intramolecular hydrogen bond as compared with OH···N.

3.C. Dimer Studies. Intermolecular hydrogen bonds are responsible for dimer formation and may influence, in a cooperative fashion, the relative strength of intramolecular hydrogen bonds present in some AE monomers (see above). The purpose of this phase of the study is to investigate possible cooperativity effects in AE dimers and to account for their magnitude and consequences using local bond orbital (NBO) theory.

3.C.1. Choice of Dimers. Thirteen minima were identified for the isolated AE molecule at the B3LYP/6-311++G(2d,2p) level of theory (see above). Combinations of them into dimers will produce several hundred possibilities. To make this study tractable, it is necessary to select a few representative structures. One of the logical candidate structures would be a dimer composed of two AE monomers in the gas-phase global minimum g′Gg′ conformation. However, on the basis of IR spectroscopic studies, Silva et al.[23] proposed that the most abundant AE conformer in the liquid phase is gGt, with a NH···O intramolecular hydrogen bond. On the basis of these findings, we selected and performed full geometry optimizations of the six AE dimers, shown in Figure 4, composed of both g′Gg′ and gGt monomers. Two of them, c1 and c2, are cyclic with two equivalent intermolecular hydrogen bonds of the OH···N (c1) or NH···O (c2) type. c1 is composed of two gGt monomers, which are distorted in the optimized complex to form the gGa/gGa dimer (a denotes anti-clinal). c2 results from two g′Gg′ conformers, which form an optimized g′Gs/g′Gs dimer (s denotes syn-periplanar). Both structures possess C2 symmetry. Four open-chain structures, o1 (gGt/gGt), o2 (g′Gg′/g′Gg′), o3 (gGt/g′Gg′), and o4 (g′Gg′/gGt) with four possible types of intermolecular hydrogen bonds (OH···N, NH···O, OH···O, and NH···N, respectively), were also studied. For all of the open-chain structures, unit 1 (on the left in Figure 4) is an intermolecular hydrogen bond donor and unit 2 (on the right in Figure 4) is an acceptor. The geometric parameters of these AE dimers are listed in Table S3 in the Supporting Information.

3.C.2. Interaction Energies. The counterpoise-corrected interaction energies, ΔE^{CP}, for AE dimers were computed at HF, B3LYP, and MP2 levels with the 6-311++G(2d,2p) basis set, by using molecular geometries optimized at the B3LYP level with the same basis set. All energetic parameters are listed in Table 4. As expected, MP2 and B3LYP interaction energies are always higher than those calculated at HF level. The difference between MP2 and B3LYP interaction energies can be attributed to dispersion interactions, which are not treated properly by DFT.[28] The effect of dispersion is more significant for dimers c2, o2, and o4 with weaker intermolecular hydrogen bonds.

BSSE (given in parentheses in Table 4) comprises up to 13% of the HF interaction energy and only up to 8% of the B3LYP interaction energy. Therefore, it appears that correction for BSSE during geometry optimization for AE dimers is not necessary, at least within our choice of basis set. However, at the MP2 level, BSSE is much higher, amounting to 13−17% of the interaction energy. Larger BSSE can be related to its overestimation by counterpoise method, which is a known problem with MP2.[55]

The trends in interaction energy are similar at all levels of theory. Dimer c1 with two OH···N intermolecular hydrogen bonds has the highest interaction energy. The formation of dimer c2 is associated with much smaller energy change. For the open-chain dimers, the interaction energy decreases in the order: o1 (OH···N) > o3 (OH···O) > o4 (NH···N) > o2 (NH···O).

The counterpoise-corrected interaction energies, ΔE^{CP}, may be further corrected by the deformation energy (E_{def}), zero-point vibrational energy, thermal energy, and entropy difference between the dimer and isolated monomers to produce values of ΔE, ΔE_0, ΔH_{dim}, and ΔG_{dim}, respectively. These corrections (see Table 4) change the stability order of AE dimers. For instance, E_{def} is relatively small for open-chain dimers (3.0−5.5% of ΔE^{CP}) but much more significant for cyclic ones (13.5 and 18.6% of ΔE^{CP} for c1 and c2, respectively), reducing the relative stability of c1 and c2. The inclusion of the entropic factor makes cyclic dimers even less favorable than corresponding open-chain forms, which is reflected in similar values of ΔG_{dim} for c1 and o1, even though c1 is enthalpically favored by 3.9 kcal/mol.

The dipole moments (Table 4) for AE dimers calculated at B3LYP level indicate that both cyclic dimers are essentially nonpolar. Open-chain dimers, however, have substantial dipole moments. Furthermore, for open-chain structures, a substantial increase in the value of the calculated dipole moment μ (up to 93% for the o1 dimer) relative to the result of vector addition of the dipole moments of subunits (in the geometry of the

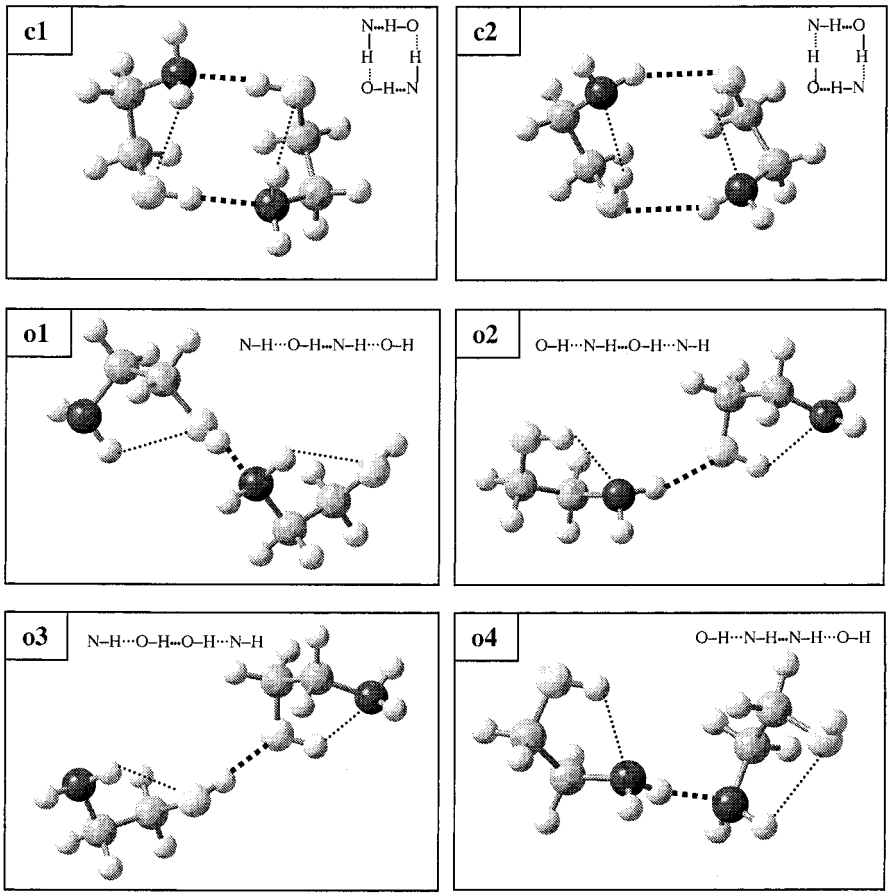

Figure 4. Selected cyclic (c1 and c2) and open-chain (o1, o2, o3, and o4) AE dimers optimized at the B3LYP/6-311++G(2d,2p) level. Both intra- and intermolecular hydrogen bonds are indicated by dotted lines, which are thicker for intermolecular hydrogen bonds. Unit 1 in each dimer is shown on the left.

TABLE 4: Energies and Dipole Moments for Selected 2-Aminoethanol Dimers, as Calculated Using B3LYP/6-311++G(2d, 2p) Optimized Geometries at HF, B3LYP and MP2 Levels of Theory and the Same Basis Set for Single Point Energy Calculations

	cyclic dimers		open chain dimers			
	c1	c2	o1	o2	o3	o4
hydrogen bond	2 OH···N	2 NH···O	OH···N	NH···O	OH···O	NH···N
HF[a,c]						
ΔE^{CP} (BSSE)[b]	−8.6 (0.8)	−3.0 (0.5)	−5.4 (0.4)	−2.7 (0.3)	−4.7 (0.4)	−2.6 (0.3)
MP2[a,c]						
ΔE^{CP} (BSSE)[b]	−15.1 (2.5)	−6.4 (1.3)	−8.5 (1.3)	−4.5 (0.9)	−6.7 (1.2)	−5.1 (0.9)
B3LYP[a,c]						
ΔE^{CP} (BSSE)[b]	−13.2 (0.7)	−4.2 (0.4)	−7.4 (0.4)	−3.4 (0.2)	−5.9 (0.4)	−3.8 (0.2)
ΔE (E_{def})[d]	−11.4 (1.8)	−3.4 (0.8)	−7.0 (0.4)	−3.3 (0.1)	−5.6 (0.2)	−3.7 (0.1)
ΔE_0[e]	−8.8	−2.2	−5.5	−2.4	−4.3	−2.6
ΔH_{dim}[f]	−9.2	−1.9	−5.3	−1.8	−3.9	−2.1
ΔG_{dim}[f]	3.2	8.1	3.2	5.3	3.7	5.7
μ (μ')[g]	0.11 (0.26)	0.99 (1.02)	1.88 (0.98)	4.75 (4.07)	3.83 (2.82)	2.85 (2.34)

[a] All energies are in kilocalories per mole. [b]Basis set superposition error (BSSE) is given in parentheses. [c]All thermodynamic parameters are counterpoise corrected. [d]ΔE is the sum of counterpoise-corrected interaction energy, ΔE^{CP}, and the deformation energy, E_{def}, given in parentheses. [e]Zero-point corrected ΔE. [f]Counterpoise-corrected enthalpy change (ΔH_{dim}) and Gibbs free energy change (ΔG_{dim}) for dimer formation are calculated at 298.15 K. [g]Dipole moments (μ and μ') are in debyes. μ', given in parentheses, is obtained by the vector addition of dipole moments of separate molecular units in geometry of the dimer calculated at the basis set of the complex.

complex), μ', is observed. This is indicative of the nonadditive (cooperative) character of the interaction.

The formation of structures similar to o1 with a relatively strong intermolecular OH···N hydrogen bond is most likely to occur in condensed, polar media (either neat liquid AE or in solution with a polar solvent). The formation of a cyclic dimer limits the extension of the intermolecular hydrogen-bonding network. Open-chain dimers, however, can be initiation sites of longer chains bonded by intermolecular interactions in a cooperative fashion. In nonpolar solvents, the formation of cyclic AE dimer arrangements, with negligible values of dipole moment, however, cannot be discarded.

In aqueous AE solution, the situation is much more complicated because of the competing hydrogen bonds with water molecules.[7] More computational studies, which are outside the scope of this work, are necessary to enumerate relevant structures of such clusters for the aqueous solutions.

3.C.3. Structural and Energetic Parameters of the Intermolecular Hydrogen Bond. The structural and energetic parameters associated with formation of both inter- and intramolecular

TABLE 5: Values for Structural and Energetic Parameters Associated with Hydrogen Bond Formation for Selected 2-Aminoethanol Dimers. B3LYP/6-311++G(2d, 2p)// B3LYP/6-311++G(2d, 2p) Calculations

	c1	c2	o1	o2	o3	o4
			intermolecular hydrogen bond			
AH···B	2 OH···N	2 NH···O	OH···N	NH···O	OH···O	NH···N
			structural parameters[a]			
r(A···B)	2.897	3.222	2.879	3.114	2.844	3.239
r(H···B)	1.922	2.362	1.908	2.123	1.880	2.229
∠(A—H···B)	172.8	141.9	170.9	165.0	172.0	170.8
			energetic parameters[b]			
n(B)→σ*(AH)						
$S(n,\sigma^*)$[c]	−0.348	0.045/0.093	0.357	0.132/0.124	0.118/0.240	0.228
$\Delta\epsilon(n,\sigma^*)$, au[d]	0.81	1.05/0.74	0.81	1.09/0.80	1.05/0.85	0.81
$E^{(2)}$, kcal/mol	15.2	0.22/1.50	15.4	1.93/1.89	2.26/7.97	5.47
n(B)↔σ(AH)						
$S(n,\sigma)$[c]	−0.187	0.020/0.064	0.195	0.076/0.075	0.059/0.133	0.139
d$E(n,\sigma)$[e]	9.62	0.17/1.21	10.4	1.85/1.52	1.24/5.36	4.58
$E_{del}(n\rightarrow\sigma^*)$[f]	19.65	2.00	19.79	4.42	11.62	6.88
$E_{del}(1\rightarrow2)$[g]	22.26	5.05	2.56	1.22	1.91	1.91
$E_{del}(2\rightarrow1)$[g]	22.26	5.05	20.39	6.06	12.93	8.25
$E_{del}(1\leftrightarrow2)$[g]	43.77	9.97	22.64	7.22	14.64	10.03
$E_{XC}(1\leftrightarrow2)$[h]	20.59	4.18	10.85	3.62	6.91	4.91
			intramolecular hydrogen bond, unit 1			
AH···B	NH···O	OH··N	NH···O	OH···N	NH···O	OH···N
			structural parameters[a]			
r(A···B)	2.861	2.753	2.871	2.797	2.866	2.802
r(H···B)	2.584	2.147	2.496	2.228	2.496	2.235
∠(A—H···B)	95.2	119.1	101.3	116.5	100.9	116.3
			energetic parameters[b]			
$E^{(2)}$, kcal/mol	0.00/0.23	3.86	0.08/0.27	2.92	0.09/0.21	2.80
$E_{del}(n\rightarrow\sigma^*)$[f]	0.27	4.92	0.41	3.72	0.35	3.58
			intramolecular hydrogen bond, unit 2			
AH···B	NH···O	OH··N	NH···O	OH···N	OH···N	NH···O
			structural parameters[a]			
r(A···B)	2.861	2.753	2.855	2.797	2.780	2.859
r(H···B)	2.584	2.147	2.487	2.242	2.212	2.497
∠(A—H···B)	95.2	119.1	100.7	115.4	116.3	100.3
			energetic parameters[b]			
$E^{(2)}$, kcal/mol	0.00/0.23	3.86	0.08/0.23	2.52	2.96	0.08/0.19
$E_{del}(n\rightarrow\sigma^*)$[f]	0.27	4.92	0.35	3.21	3.78	0.30

[a] All distances are in angstroms; angles are in degrees. [b]For conformers with the NH···O and OH···O inter- or intramolecular hydrogen bonds, the charge transfer and exchange repulsion with both lone pairs on the oxygen atom are given and separated by a slash in the order n_{sp}(O)/n_p(O). [c]Overlap integral of associated pre-orthogonalized NBOs. [d]NBO energy difference between n and σ^*. [e]Pairwise exclusion repulsion energy (in kilocalories per mole) between n and σ. [f]Energy change (in kilocalories per mole) associated with deletion of off-diagonal matrix elements of the effective one-electron Hamiltonian corresponding to either one or two remote $n(B)\rightarrow\sigma^*(AH)$ charge-transfer interactions. [g]Energy changes (in kilocalories per mole) associated with deletion of intermolecular CT interactions between units 1 and 2: in one direction, $E_{del}(1\rightarrow2)$ and $E_{del}(2\rightarrow1)$; in both directions, $E_{del}(1\leftrightarrow2)$. [h]Sum of intermolecular pairwise steric exchange energies (in kilocalories per mole).

hydrogen bonds in AE dimers are given in Table 5. The data demonstrate that an intermolecular hydrogen bond is stronger and more linear than the corresponding intramolecular interaction. Among open-chain dimers, dimer o3 has the most linear intermolecular hydrogen bond (deviation from 180° is just 8°) and the smallest internuclear distance H···B (1.880 Å). This is an indication that the OH···O hydrogen bond is the strongest one, which is in contradiction with the trends in interaction energies. Energetic analysis based on NBO theory, however, can clarify this situation.

The values of the energy lowering associated with remote n(B)→σ*(AH) delocalizations, calculated as $E^{(2)}$ estimates (Table 4), demonstrate that intermolecular CT interactions for dimers are much more favorable than corresponding intramolecular interactions for AE monomers. For instance, an increase in the remote n(N)→σ*(OH) delocalization by a factor of 7.7 for the o1 dimer (intermolecular) compared with the corresponding estimate for the g′Gg′ monomer equilibrium structure (intramolecular) is observed. The nature of the orbital overlap associated with intermolecular hydrogen bond formation for open-chain dimers is shown in Figure 5. From this figure and from the numbers in Table 5, it is clear that the overlap and the corresponding CT are the strongest for the o1 dimer with an OH···N intermolecular hydrogen bond. In this case, the antibonding σ*(OH) orbital becomes even more asymmetric and more polarized toward hydrogen than found for the intramolecular hydrogen bond formation of this type (cf. Figures 2 and 5). The unfavorable overlap between n(B) and σ(AH), $S(n,\sigma)$, is smaller than $S(n,\sigma^*)$ for all dimers. This indicates that the n(B)→σ*(AH) delocalization easily overcomes unfavorable n(B)↔σ(AH) exchange repulsion.

To compare the relative strength of intermolecular hydrogen bonds of different types, deletion energies, $E_{del}(n\rightarrow\sigma^*)$, listed in Table 5, for the intermolecular n(B)→σ*(AH) CT were calculated. For open-chain dimers the ranking by $E_{del}(n\rightarrow\sigma^*)$ agrees with that obtained by the interaction energy. AE dimer

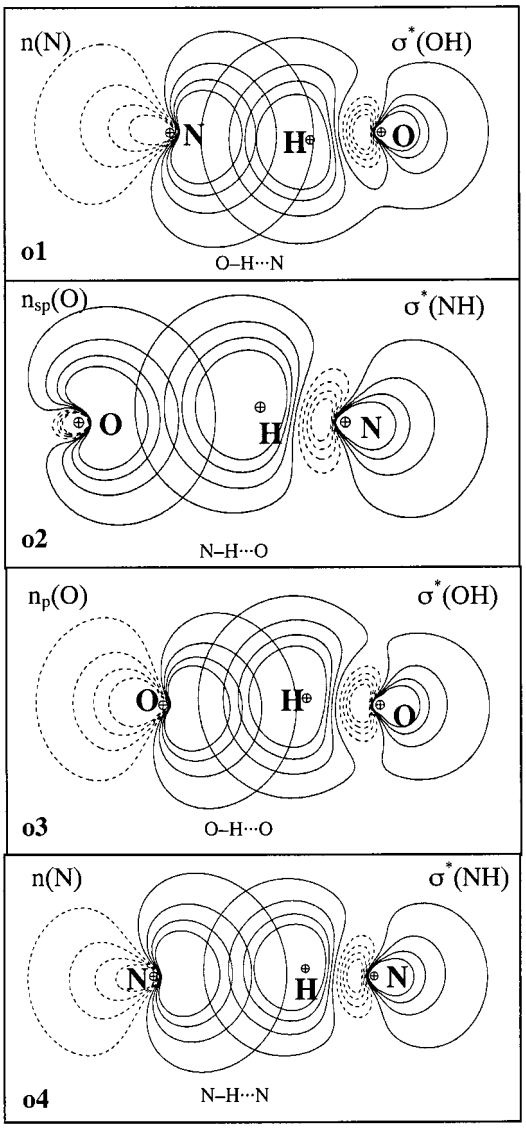

Figure 5. Contour plots of the overlap of pre-NBOs of lone pair n(B) of unit 2 with antibonding orbital σ^*(AH) of unit 1 associated with intermolecular AH···B hydrogen bond formation (A and B are oxygen or nitrogen) for four open-chain AE dimers o1, o2, o3, and o4. B3LYP/6-311++G(2d,2p)//B3LYP/6-311++G(2d,2p) calculations. Atomic positions are indicated by circled crosses. The relative positions of atoms are the same on both plots. The outermost contours are at 0.032 au, and the contour interval is 0.05 au.

o1 therefore has the strongest intermolecular hydrogen bond, which was not clear from structural parameters alone.

For all open-chain structures, $E_{del}(n\rightarrow\sigma^*)$ comprises a substantial fraction of the deletion energy of all CT interactions going from unit 2 to unit 1, $E_{del}(2\rightarrow1)$: from about 73% for o2 up to about 97% for o1. Intermolecular CT interactions going from unit 1 to unit 2, estimated by $E_{del}(1\rightarrow2)$, are much weaker and mostly represent back-donations from n(A) to Rydberg orbitals of B. Therefore, remote n(B)$\rightarrow\sigma^*$(AH) delocalizations associated with the formation of the hydrogen bond are the strongest intermolecular CT interactions of all and comprise about 61−87% of the energy lowering associated with CT between units 1 and 2 in both directions, $E_{del}(1\leftrightarrow2)$. The trend in $E_{del}(1\leftrightarrow2)$ for all dimers follows that for the interaction energy, demonstrating the importance of CT interactions in the stabilization of AE dimers. The sum of pairwise steric exchange repulsions between two units, $E_{XC}(1\leftrightarrow2)$, is always smaller than $E_{del}(1\leftrightarrow2)$, which again confirms that hydrogen-bonding interactions overcome unfavorable repulsions between the two units.

3.C.4. Changes in Structural and Vibrational Parameters Associated with Intermolecular Hydrogen Bond Formation. The formation of an intermolecular hydrogen bond in AE dimers causes changes in structural parameters within the AE units. Most distinct is the lengthening of the O−H or N−H bond and red shifts in the frequency of ν(OH) or $\nu_s(NH_2)$ and $\nu_{as}(NH_2)$ vibrations for the hydrogen bond donor unit compared with the isolated AE molecule. The effect is most dramatic for dimers c1 and o1 with the strongest OH···N intermolecular hydrogen bond: the O−H bond is lengthened by 0.021 and 0.019 Å, respectively, and the frequency of ν(OH) is red-shifted by 403 and 399 cm^{-1}, respectively (compared with the isolated gGt conformer). Corresponding changes are smaller for dimer o3 with the OH···O intermolecular interaction. For the NH···N hydrogen-bonded dimer o4, the lengthening of the N−H bond (0.007 Å) and the red shifts in $\nu_s(NH_2)$ and $\nu_{as}(NH_2)$ (91 and 45 cm^{-1}, respectively) are the greatest, but less substantial.

As in hydrogen-bonded AE monomers, these bond length changes and frequency shifts can be explained by the weakening of the corresponding O−H or N−H bond because of n(B)$\rightarrow\sigma^*$(AH) intermolecular CT. For dimers c1 and o1 (unit 1 of the latter), the occupancy of σ^*(OH) increases by almost an order of magnitude, and the NRT bond order of this O−H bond decreases (by 0.021 and 0.020, respectively) relative to the isolated gGt conformer. The weakening of the N−H bond for dimers o4, o2, and c2 is associated with the increased occupancy of the corresponding σ^*(NH) (by a factor of 3.5 for o4) and the decrease in the NRT bond order (by 0.008 for o4) in comparison with g′Gg′.

A dramatic increase in the infrared intensity for these modes of vibrations is observed also. The IR intensity of ν(OH) for c1 and o1 dimers is increased by a factor of 44 and 28, respectively, compared with the isolated gGt monomer. The increase in IR intensity for $\nu_s(NH_2)$ is even more dramatic: 583-fold for o4 and 307-fold for o2 dimers in comparison with g′Gg′. The corresponding increase for $\nu_{as}(NH_2)$ is much smaller: 13-fold for o2 and 6.4-fold for o4. The explanation of this IR intensity increase is the same as in the AE monomers with the intramolecular hydrogen bond (see above). For the dimer, however, this effect is much more pronounced because of the greater intermolecular CT that results in greater polarization of the O−H or N−H bond. For instance, the polarization of σ(OH) toward oxygen in c1 is increased by 3.3% relative to the gGt conformer. This enhanced polarization produces larger dipole difference with respect to the same displacement, thereby resulting in a more substantial increase in IR intensity.

The substantial red shift in the frequency and IR intensity increase of the ν(OH) normal mode of vibration for dimers compared with the isolated AE molecule are in good agreement with infrared spectroscopic data on the neat liquid AE.[23] When scaled by a factor of 0.9613,[53] the calculated value for the frequency of ν(OH) for AE dimers with the OH···N intermolecular hydrogen bond (e.g., 3326 cm^{-1} for the o1 dimer) is close to the experimental value[23] of 3347 cm^{-1}. Peaks for $\nu_s(NH_2)$ and $\nu_{as}(NH_2)$ were not distinguishable in the IR spectrum of liquid AE.[23]

The intermolecular n(B)$\rightarrow\sigma^*$(AH) delocalization in AE dimers modulates vicinal CT interactions of both donor and acceptor lone pairs in a fashion similar to that described for the hydrogen-bonded AE monomers (see above). This can be confirmed by the changes in C−O and C−N bond lengths for AE dimers compared with the equilibrium monomer structures.

For example, for unit 1 of the o1 dimer, C−O is shortened by 0.011 Å, which is due to an increase (relative to gGt) in vicinal delocalizations from both n(O)s by 3.2 kcal/mol. The NRT bond order of C−O increases slightly (by 0.005 compared with gGt). For all open-chain dimers studied, the overall enhancement of vicinal CT interactions from both oxygen and nitrogen lone pairs of the hydrogen bond donor unit (unit 1) is observed. The opposite is true for the acceptor unit (unit 2) of these dimers.

Changes in structural parameters are the most dramatic for cyclic dimers (cf. values in Tables S1 and S3). This is reflected in substantial values of the deformation energy, E_{def}, for these structures (see above) and also in the decrease in the deletion energy of all $\sigma\rightarrow\sigma^*$ CT interactions of the molecular subunit of the complex compared with the equilibrium monomer structure (by 2.9 kcal/mol for each subunit of c1 dimer). However, this decrease is overcome by the increase in vicinal delocalizations of lone pairs on oxygen and nitrogen atoms also mentioned above.

As a result of the structural distortion which brings on close Lewis orbital contacts, unfavorable steric exchange repulsions are intensified for molecular units of AE dimers compared with the isolated AE monomers. The most substantial increase is also observed for the cyclic c1 dimer. The difference in total steric exchange energy between each subunit of the dimer and equilibrium monomer structure is 27.3 kcal/mol in this case.

3.C.5. Enhancement of the Intramolecular Hydrogen Bond: Cooperativity in the Interaction. The comparison of structural parameters associated with an intramolecular hydrogen bond formation for AE monomers (Table 3) and dimers (Table 5) demonstrates that an enhancement of this interaction takes place upon dimerization of AE monomers. The intramolecular OH···N hydrogen bond for the cyclic dimer c2 is strengthened the most. This is reflected by the decrease in the H···N distance by 0.146 Å and the widening of O−H···N angle by 5.1° toward the "ideal" 180°. For the c2 dimer, $E_{del}(n\rightarrow\sigma^*)$ associated with the intramolecular OH···N interaction increases by a factor of 1.9 compared with the isolated g′Gg′ conformer. A substantial enhancement of the NH···O intramolecular hydrogen bond is observed also for unit 1 of the o1 dimer, as indicated by an increase in $E_{del}(n\rightarrow\sigma^*)$ by a factor of 1.7 as compared with gGt. The reinforcement of this interaction for the other unit of this dimer is somewhat smaller, a factor of 1.5. The changes in structural and vibrational parameters compared with the monomer values also confirm the enhancement of intramolecular n(B)→σ^*(AH) CT interactions occurring in AE dimers. These changes are the most significant for the c2 dimer: the O−H bond is lengthened by 0.004 Å, the angle C−O−H is contracted by 1.0°, the frequency of ν(OH) is red-shifted by 77 cm^{-1}, and its IR intensity is increased by a factor of 1.7 (all relative to corresponding values for g′Gg′).

The reinforcement of intramolecular hydrogen bond in AE dimers is a cooperative phenomenon which, as pointed out in studies by the Weinhold group,[29,37,41] cannot be explained by the electrostatic nature of hydrogen-bonding interactions. Unlike electrostatics, CT interactions are nonadditive and may enhance each other in the cooperative fashion.[29] This is also found in our theoretical studies of small AE clusters. For instance, as a consequence of the intermolecular n(N)→σ^*(OH) CT, the energy of the n_{sp}(O) orbital of unit 1 of the o1 dimer is increased by 0.056 au and its s-character is decreased by 4.1% making it more diffuse (compared with the isolated gGt monomer). For the other unit of this dimer, the energy of σ^*(NH) is decreased by 0.023 au and its polarization toward hydrogen is increased by 0.6% (relative to gGt). Therefore, the intramolecular remote n(O)→σ^*(NH) CT is increased in both cases (cf. $E^{(2)}$ values in Tables 3 and 5). Similar changes in energies and hybrid compositions are observed for other dimers. Thus, NBO analysis directly shows that the cooperative nature of CT interactions enhances intramolecular hydrogen bonding in AE dimers.

The theoretical study of AE dimers is the first and important step for the understanding of forces that govern the aggregation of this molecule in the liquid phase or concentrated solution. The results, in particular, may be used for the description of liquid AE in the framework of quantum cluster equilibrium (QCE) theory of Weinhold and co-workers.[68]

4. Conclusions

The conformational analysis performed at the B3LYP/6-311++G(2d,2p) level for stable conformers of AE demonstrated that the formation of OH···N or NH···O intramolecular hydrogen bonds enhances the stability of AE conformers, produces the lengthening of corresponding bonds (OH or NH), contraction of bond angles (COH or CNH), red shifts and IR intensity increases of corresponding normal modes of vibration, ν(OH) or $\boldsymbol{\nu}(NH_2)$. NBO analysis shows these changes are a consequence of remote $n\rightarrow\sigma^*$ electron delocalizations, which bring electron density from the lone pair of the hydrogen bond acceptor into the antibonding orbital of the donor. These energetically favorable charge-transfer interactions are the strongest for the global minimum, OH···N hydrogen-bonded g′Gg′ conformer, in full agreement with the trends in structural and vibrational parameters. On the other hand, NH···O type hydrogen bonds are much weaker, and the stabilizing effect of remote n(O)→σ^*(NH) delocalizations is mostly counteracted by opposing stereoelectronic effects. The increased stability of all AE conformers with the intramolecular hydrogen bond can be explained by the cooperative enhancement of vicinal $n\rightarrow\sigma^*$ charge transfer as a consequence of electron density redistribution caused by remote delocalizations associated with hydrogen-bonding interactions.

The bent nature of the intramolecular hydrogen bonds in AE monomers results in the increase in steric exchange repulsion and consequent weakening of these interactions. Therefore, they can be easily overcome by stronger and more linear intermolecular hydrogen bonds in the condensed phase, where association of AE molecules takes place. This has been shown experimentally and is confirmed by our computational study on the set of AE dimers.

As expected, the formation of intermolecular hydrogen bonds is the main stabilizing factor in the dimerization of AE monomers. Open-chain structures with the strongest OH···N intermolecular interaction are most likely to be formed in polar condensed media. For all AE dimers the stabilizing charge-transfer component of the intermolecular hydrogen bond attributed to remote $n\rightarrow\sigma^*$ delocalizations is much greater than corresponding parameter for the intramolecular interactions in AE monomers. Associated structural and vibrational changes with respect to AE monomer values correlate well with the NBO estimate of the hydrogen bond strength.

Some internal delocalizations are enhanced as a consequence of the intermolecular $n\rightarrow\sigma^*$ charge transfer. For instance, the reinforcement of the intramolecular hydrogen bond in both molecular units of any AE dimer by as much as 1.9-fold is also observed. The cooperative character of the intra- and intermolecular hydrogen-bonding interactions in AE clusters is caused by the substantial and inherently nonadditive charge transfer component. One may expect that such cooperative reinforcement of the intermolecular hydrogen bonds in extended AE chains

also takes place. This may be a field for future studies that eventually lead to the better understanding of the nature of forces that govern aggregation of AE and similar molecules and, therefore, a better physical-chemical description of such systems.

Acknowledgment. We gratefully acknowledge the support of the National Eye Institute of the National Institutes of Health (grant EY11657). Computer time allocations were received from the National Computational Science Alliance under grants CHE98008N and CHE990012N and the Advanced Biomedical Computing Center of the Frederick Cancer Research and Development Center, National Institutes of Health.

Supporting Information Available: Three tables of most important geometric parameters for 2-aminoethanol monomers and dimers as well as ethanol and ethylamine monomers are given as Supporting Information. This material is available free of charge via the Internet at http://pubs.acs.org.

References and Notes

(1) Edlund, U.; Holloway, C.; Levy, G. C. *J. Am. Chem. Soc*. **1976,** *98*, 5069.
(2) El-Bermani, M. F. *J. Iraqi Chem. Soc.* **1976,** *1*, 19.
(3) Kharitonov, I. J.; Khoshabova, E. G.; Rodnikova, M. N.; Dudnikova, K. T.; Razumova, A. B. *Dokl. Akad. Nauk SSSR* **1989,** *304*, 917.
(4) Kharitonov, Y. Y.; Khoshabova, E. G.; Rodnikova, M. N. *Bull. Acad. Sci. USSR Div. Chem. Sci.* **1990,** *39*, 1190.
(5) Krueger, P. J.; Mettee, H. D. *Can. J. Chem.* **1965,** *43*, 2970.
(6) Leavell, S.; Steichen, J.; Franklin, J. L. *J. Chem. Phys.* **1973,** *59*, 4343.
(7) Mate-Divo, M.; Barcza, L. *Z. Phys. Chem.* **1995,** *190*, 223.
(8) Penn, R. E.; Curl, R. F. *J. Chem. Phys.* **1971,** *55*, 651.
(9) Penn, R. E.; Olsen, R. J. *J. Mol. Spectrosc.* **1976,** *62*, 423.
(10) Rodnikova, M. N.; Privalov, V. I.; Samigullin, F. M.; Zhakova, V. V. *Zh. Fiz. Khim.* **1994,** *68*, 2235.
(11) Mootz, D.; Brodalla, D.; Wiebcke, M. *Acta Crystallogr. Sect. C: Cryst. Struct. Commun.* **1989,** *45*, 754.
(12) Alejandre, J.; Rivera, J. L.; Mora, M. A.; de la Garza, V. *J. Phys. Chem. B* **2000,** *104*, 1332.
(13) Buemi, G. *Int. J. Quantum Chem.* **1996,** *59*, 227.
(14) Button, J. K.; Gubbins, K. E.; Tanaka, H.; Nakanishi, K. *Fluid Phase Equilib.* **1996,** *116*, 320.
(15) Chang, Y. P.; Su, T. M.; Li, T. W.; Chao, I. *J. Phys. Chem. A* **1997,** *101*, 6107.
(16) Kelterer, A. M.; Ramek, M.; Frey, R. F.; Cao, M.; Schafer, L. *THEOCHEM J. Mol. Struct.* **1994,** *310*, 45.
(17) Kelterer, A. M.; Ramek, M. *THEOCHEM J. Mol. Struct.* **1991,** *232*, 189.
(18) Millefiori, S.; Raudino, A.; Zuccarello, F. *Z. Phys. Chem. (Wiesbaden)* **1980,** *123*, 67.
(19) Radom, L.; Lathan, W. A.; Hehre, W. J.; Pople, J. A. *J. Am. Chem. Soc.* **1973,** *95*, 693.
(20) Raudino, A.; Millefiori, S.; Zuccarello, F.; Millefiori, A. *J. Mol. Struct.* **1979,** *51*, 295.
(21) Van Alsenoy, C.; Siam, K.; Ewbank, J. D.; Schafer, L. *THEOCHEM J. Mol. Struct.* **1986,** *136*, 77.
(22) Vanquickenborne, L. G.; Coussens, B.; Verlinde, C.; De Ranter, C. *THEOCHEM J. Mol. Struct.* **1989,** *201*, 1.
(23) Silva, C. F. P.; Duarte, M. L.; Fausto, R. *J. Mol. Struct.* **1999,** *483*, 591.
(24) Rasanen, M.; Aspiala, A.; Homanen, L.; Murto, J. *J. Mol. Struct.* **1982,** *96*, 81.
(25) Cabaleiro-Lago, E. M.; Rios, M. A. *J. Phys. Chem. A* **1999,** *103*, 6468.
(26) Cabaleiro-Lago, E. M.; Rios, M. A. *J. Chem. Phys.* **2000,** *113*, 9523.
(27) Sum, A. K.; Sandler, S. I. *J. Phys. Chem. A* **2000,** *104*, 1121.
(28) Hobza, P.; Sponer, J.; Reschel, T. *J. Comput. Chem.* **1995,** *16*, 1315.
(29) King, B. F.; Weinhold, F. *J. Chem. Phys.* **1995,** *103*, 333.
(30) Cabaleiro-Lago, E. M.; Rios, M. A. *J. Chem. Phys.* **2000,** *112*, 2155.
(31) Levy, J. B.; Martin, N. H.; Hargittai, I.; Hargittai, M. *J. Phys. Chem. A* **1998,** *102*, 274.
(32) Luque, F. J.; Lopez, J. M.; de la Paz, M. L.; Vicent, C.; Orozco, M. *J. Phys. Chem. A* **1998,** *102*, 6690.
(33) Taurian, O. E.; Contreras, R. H. *THEOCHEM J. Mol. Struct.* **2000,** *504*, 119.
(34) Wong, N. B.; Cheung, Y. S.; Wu, D. Y.; Ren, Y.; Tian, A. M.; Li, W. K. *J. Phys. Chem. A* **2000,** *104*, 6077.
(35) Wong, N. B.; Cheung, Y. S.; Wu, D. Y.; Ren, Y.; Wang, X.; Tian, A. M.; Li, W. K. *THEOCHEM J. Mol. Struct.* **2000,** *507*, 153.
(36) Peralta, J. E.; de Azua, M. C. R.; Contreras, R. H. *THEOCHEM J. Mol. Struct.* **1999,** *491*, 23.
(37) Reed, A. E.; Curtiss, L. A.; Weinhold, F. *Chem. Rev.* **1988,** *88*, 899.
(38) Reed, A. E.; Weinhold, F. *J. Chem. Phys.* **1983,** *78*, 4066.
(39) Reed, A. E.; Weinhold, F.; Curtiss, L. A.; Pochatko, D. J. *J. Chem. Phys.* **1986,** *84*, 5687.
(40) Novak, P.; Vikictopic, D.; Meic, Z.; Sekusak, S.; Sabljic, A. *J. Mol. Struct.* **1995,** *356*, 131.
(41) Weinhold, F. *THEOCHEM J. Mol. Struct.* **1997,** *398*, 181.
(42) Frisch, M. J.; Trucks, G. W.; Schlegel, H. B.; Scuseria, G. E.; Robb, M. A.; Cheeseman, J. R.; Zakrzewski, V. G.; Montgomery, J. A., Jr.; Stratmann, R. E.; Burant, J. C.; Dapprich, S.; Millam, J. M.; Daniels, A. D.; Kudin, K. N.; Strain, M. C.; Farkas, O.; Tomasi, J.; Barone, V.; Cossi, M.; Cammi, R.; Mennucci, B.; Pomelli, C.; Adamo, C.; Clifford, S.; Ochterski, J.; Petersson, G. A.; Ayala, P. Y.; Cui, Q.; Morokuma, K.; Malick, D. K.; Rabuck, A. D.; Raghavachari, K.; Foresman, J. B.; Cioslowski, J.; Ortiz, J. V.; Stefanov, B. B.; Liu, G.; Liashenko, A.; Piskorz, P.; Komaromi, I.; Gomperts, R.; Martin, R. L.; Fox, D. J.; Keith, T.; Al-Laham, M. A.; Peng, C. Y.; Nanayakkara, A.; Gonzalez, C.; Challacombe, M.; Gill, P. M. W.; Johnson, B.; Chen, W.; Wong, M. W.; Andres, J. L.; Gonzalez, C.; Head-Gordon, M.; Replogle, E. S.; Pople, J. A. *Gaussian 98*, Revision A.6; Gaussian, Inc.: Pittsburgh, PA, 1998.
(43) Becke, A. D. *J. Chem. Phys.* **1993,** *98*, 5648.
(44) Lee, C. T.; Yang, W. T.; Parr, R. G. *Phys. Rev. B* **1988,** *37*, 785.
(45) Latajka, Z.; Bouteiller, Y. *J. Chem. Phys.* **1994,** *101*, 9793.
(46) Muller-Dethlefs, K.; Hobza, P. *Chem. Rev.* **2000,** *100*, 143.
(47) Frisch, M. J.; Scheiner, A. C.; Schaefer, H. F.; Binkley, J. S. *J. Chem. Phys.* **1985,** *82*, 4194.
(48) Chung, G.; Kwon, O.; Kwon, Y. *J. Phys. Chem. A* **1998,** *102*, 2381.
(49) Masella, M.; Flament, J. P. *J. Chem. Phys.* **1999,** *110*, 7245.
(50) Lii, J. H.; Ma, B. Y.; Allinger, N. L. *J. Comput. Chem.* **1999,** *20*, 1593.
(51) Lundell, J.; Latajka, Z. *J. Phys. Chem. A* **1997,** *101*, 5004.
(52) Lundell, J.; Latajka, Z. *Chem. Phys.* **2001,** *263*, 221.
(53) Przeslawska, M.; Melikowa, S. M.; Lipkowski, P.; Koll, A. *Vib. Spectrosc.* **1999,** *20*, 69.
(54) Boys, S. F.; Bernardi, F. *Mol. Phys.* **1970,** *19*, 553.
(55) Cook, D. B.; Sordo, J. A.; Sordo, T. L. *Int. J. Quantum Chem.* **1993,** *48*, 375.
(56) Weinhold, F. Natural Bond Orbital Methods. In *Encyclopedia of Computational Chemistry*; Schleyer, P. v. R., Allinger, N. L., Clark, T., Gasteiger, J., Kollman, P. A., Schaefer, H. F., III, Schreiner, P. R., Eds.; John Wiley & Sons: Chichester, 1998; Vol. 3; p 1792.
(57) Reed, A. E.; Weinstock, R. B.; Weinhold, F. *J. Chem. Phys.* **1985,** *83*, 735.
(58) Badenhoop, J. K.; Weinhold, F. *J. Chem. Phys.* **1997,** *107*, 5406.
(59) Feldgus, S.; Landis, C. R.; Glendening, E. D.; Weinhold, F. *J. Comput. Chem.* **2000,** *21*, 411.
(60) Glendening, E. D.; Badenhoop, J. K.; Weinhold, F. *J. Comput. Chem.* **1998,** *19*, 628.
(61) Glendening, E. D.; Weinhold, F. *J. Comput. Chem.* **1998,** *19*, 593.
(62) Glendening, E. D.; Weinhold, F. *J. Comput. Chem.* **1998,** *19*, 610.
(63) Weinhold, F. *NBO 4.0 Program Manual*; Theoretical Chemistry Institute: University of Wisconsin, Madison, 1996.
(64) Fletcher, R.; Powell, M. J. D. *Comput. J.* **1963,** *6*, 163.
(65) Bondi, A. *J. Phys. Chem.* **1964,** *68*, 441.
(66) Harmony, M. D.; Laurie, V. W.; Kuczkowski, R. L.; Schwendeman, R. H.; Ramsay, D. A.; Lovas, F. J.; Lafferty, W. J.; Maki, A. G. *J. Phys. Chem. Ref. Data* **1979,** *8*, 619.
(67) Varnali, T.; Hargittai, I. *THEOCHEM J. Mol. Struct.* **1996,** *388*, 315.
(68) Weinhold, F. *J. Chem. Phys.* **1998,** *109*, 367.